

1           **Marine-Derived Water-Soluble Organic Nitrogen in**  
2           **Coastal Air: Influence of Ocean Productivity on**  
3           **Atmospheric Nitrogen Cycling**

4  
5   Jiao Tang<sup>1,2</sup>, Shujie Hu<sup>3\*</sup>, Xiao Wang<sup>4</sup>, Jiaqi Wang<sup>5</sup>, Shaojun Lv<sup>2</sup>, Xiaofei Geng<sup>2</sup>,  
6   Guangcai Zhong<sup>2</sup>, Yangzhi Mo<sup>2</sup>, Surat Bualert<sup>6</sup>, Jun Li<sup>2</sup>, Shizhen Zhao<sup>2\*</sup>, Gan  
7   Zhang<sup>2</sup>

8  
9   <sup>1</sup>College of Marine Sciences, South China Agricultural University, Guangzhou  
10 510642, China

11 <sup>2</sup>State Key Laboratory of Advanced Environmental Technology, Guangzhou  
12 Institute of Geochemistry, Chinese Academy of Sciences, Guangzhou 510640,  
13 China

14 <sup>3</sup>Chongqing Institute of Green and Intelligent Technology, Chinese Academy of  
15 Sciences, Chongqing 400714, China

16 <sup>4</sup>School of Resources and Environment, Henan Polytechnic University, Jiaozuo  
17 454003, China

18 <sup>5</sup>School of Electrical and Information Engineering, Zhengzhou University,  
19 Zhengzhou 450001, China

20 <sup>6</sup>Faculty of Environment, Kasetsart University, Bangkok 10900, Thailand

21  
22 **\*Correspondence:** Shujie Hu (hushujie@cigit.ac.cn) and Shizhen Zhao  
23 (zhaoshizhen@gig.ac.cn)

24

25        **Abstract**

26        Organic nitrogen (ON) deposition from aerosols plays a crucial role in  
27        oceanic ecosystems; however, the influence of marine biogenic activity on  
28        atmospheric ON remains poorly understood. Here, we investigate the  
29        contribution of the marine biosphere to water-soluble ON (WSON) in coastal  
30        aerosols based on particulate matter samples collected in Bangkok, Thailand,  
31        from January 2016 to January 2017. Concentrations of WSON and water-  
32        soluble inorganic nitrogen (WSIN, including  $\text{NO}_3^-$  and  $\text{NH}_4^+$ ) were analyzed and  
33        compared across days classified by air mass origin over land as marine-,  
34        mixed-, or continental-influenced. Air masses of marine origin showed  
35        significantly lower WSON and WSIN concentrations than those from mixed and  
36        continental origins. Nevertheless, WSON remained a substantial fraction of  
37        water-soluble total nitrogen (WSTN) across all air-mass categories, although  
38        the WSON/WSTN ratio alone did not uniquely distinguish marine from  
39        anthropogenic influence. Positive matrix factorization revealed that the  
40        contribution of sea spray aerosol (SSA)-associated WSON to total WSON  
41        increased markedly with oceanic influence, accounting for  $3.8\% \pm 6.4\%$ ,  $14\% \pm$   
42         $14\%$ , and  $34\% \pm 17\%$  under continental, mixed, and marine conditions,  
43        respectively. The corresponding contributions to WSTN were approximately  $1.6\%$   
44         $\pm 2.1\%$ ,  $7.3\% \pm 7.6\%$ , and  $13\% \pm 8.2\%$ , with an overall mean of  $7.8\% \pm 8.2\%$   
45        over the sampled annual cycle. Moreover, marine productivity, assessed via air  
46        mass exposure to chlorophyll-a concentrations, exhibited a strong positive  
47        correlation with SSA-associated WSON ( $r = 0.96$ ,  $p < 0.001$ ), a pattern further  
48        supported by large-scale comparison across coastal sites. These results  
49        provide multiple lines of evidence that SSA-associated WSON is an important  
50        contributor to coastal aerosol WSON under marine influence, with patterns  
51        consistent with marine-biogenic enhancement, although anthropogenic co-  
52        influences cannot be fully excluded.

53

54

## 55           **1. Introduction**

56           Organic nitrogen (ON), which includes compounds such as amino acids,  
57           urea, organic nitrates, nitroaromatics, and humic-like substances, plays an  
58           important role in atmospheric processes including air quality, cloud formation,  
59           and the nitrogen cycle (Cape et al., 2011). On a global scale, water-soluble ON  
60           (WSON) has been estimated to contribute 10%–40% of total airborne ON  
61           (Cape et al., 2011; Liu et al., 2021; Matsumoto et al., 2019a), influencing aerosol  
62           properties such as solubility, acidity, and hygroscopicity. Furthermore, certain  
63           nitrogen-containing organic compounds, including nitroaromatics, have been  
64           recognized as important chromophores in brown carbon (He et al., 2022; Liu et  
65           al., 2023), thereby influencing radiative forcing. In addition, atmospheric  
66           deposition of particulate WSON is increasingly regarded as a significant source  
67           of nitrogen input to marine ecosystems (Buchanan et al., 2021; Li et al., 2023).

68           WSON originates from both direct emissions—including anthropogenic  
69           and biogenic sources—and secondary formation through atmospheric  
70           reactions (Xu et al., 2020; Yu et al., 2017). These complex sources and  
71           atmospheric processes contribute to substantial spatial and temporal variability  
72           in WSON deposition (Kanakidou et al., 2012; Li et al., 2023; Yu et al., 2020).  
73           Previous studies have identified marine emissions as a notable source of  
74           atmospheric ON (Facchini et al., 2008; O'Dowd et al., 2004). Globally, the  
75           estimated annual primary emission of soluble ON from the ocean is 2.1 Tg N  
76           yr<sup>-1</sup>, comparable in magnitude to anthropogenic emissions from fossil-fuel  
77           combustion and biomass burning (BB) (Ito et al., 2014; Kanakidou et al., 2012).  
78           In some remote marine regions, isotopic evidence suggests that aerosol ON  
79           can be strongly influenced by marine biological production rather than terrestrial  
80           pollution (Altieri et al., 2016).

81           Recent research has underscored the complexity and variability of WSON  
82           in sea spray aerosol (SSA) (Altieri et al., 2012; Li et al., 2019). For instance,  
83           primary sea-spray emissions have been recognized as a major source of  
84           WSON over the remote Indian sector of the Southern Ocean (Matsumoto et al.,  
85           2022). These findings highlight the importance of incorporating marine ON  
86           emissions in assessments of net atmospheric WSON deposition, particularly in  
87           the open ocean (Luo et al., 2018). However, several field studies in regions  
88           strongly influenced by marine air masses have reported only minor  
89           contributions from marine-derived WSON—typically below 5% (Leung et al.,

90 2024; Tsagkaraki et al., 2021). This discrepancy highlights the continuing  
91 challenge of distinguishing marine from anthropogenic WSON sources in  
92 coastal and adjacent marine environments. In this study, we address this issue  
93 by combining Positive Matrix Factorization (PMF) source apportionment, air-  
94 mass trajectory analysis, a trajectory-based land-retention index, and  
95 chlorophyll-a (Chl-a) exposure as complementary lines of evidence, while  
96 recognizing that these approaches reduce but do not fully eliminate source  
97 ambiguity.

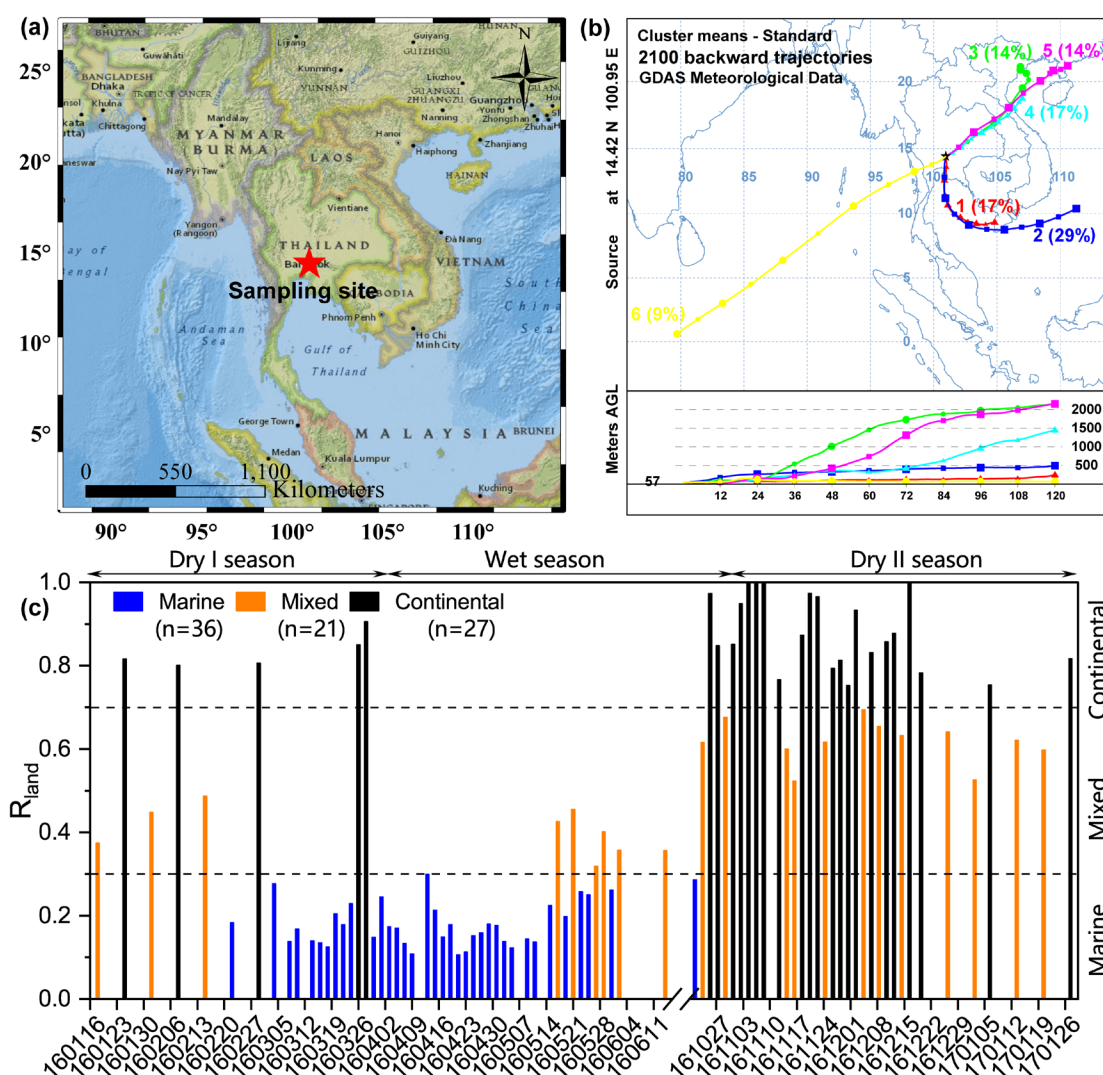
98 The Indochinese Peninsula (ICP), characterized by high population density  
99 and substantial ON deposition (Ito et al., 2014; Kanakidou et al., 2012; Li et al.,  
100 2023), provides a suitable context for assessing the influence of marine  
101 aerosols on atmospheric WSON. Eutrophication, defined as the excessive  
102 enrichment of aquatic systems by nutrients that alters ecosystem structure and  
103 function, may enhance primary productivity and potentially promote the  
104 emission of ON to the atmosphere (Altieri et al., 2016). Here, we selected  
105 Bangkok, the capital of Thailand, which is situated in the central plain of the  
106 country and adjacent to the Gulf of Thailand. The region experiences prevailing  
107 marine winds from January to October, offering a favorable setting for studying  
108 marine aerosol contributions to WSON. Our study aims to: (1) quantify WSON  
109 abundances at a coastal site in the ICP; (2) assess marine influences on WSON  
110 distributions; and (3) elucidate the mechanisms governing oceanic  
111 contributions to WSON.

## 112 **2. Material and Methods**

### 113 **2.1. Sampling Campaign**

114 A total of 84 total suspended particulate (TSP) samples were collected from  
115 the rooftop (57 m above ground level) of the Faculty of Environment at  
116 Kasetsart University (100°57' E and 13°85' N; Figure 1a) in Bangkok,  
117 Thailand—a site previously characterized in air quality studies (Tang et al., 2021;  
118 Wang et al., 2020). Sampling was conducted over 24-hour periods using a high-  
119 volume air sampler (flow rate: 0.3 m<sup>3</sup> min<sup>-1</sup>) equipped with pre-combusted  
120 quartz-fiber filters (450 °C for 6 h). The collection period spanned from 18  
121 January 2016 to 28 January 2017, covering three distinct seasons: Dry I  
122 (January–March 2016, n = 19), Wet (April–June and October 2016, n = 35), and  
123 Dry II (November 2016–January 2017, n = 30). Sampling frequency averaged  
124 5 ± 2 days per month during January–February 2016 and January 2017, with

125 intensified campaigns in March–May and late October–December. Sampling  
 126 was limited between June and October due to heavy rainfall. Because the  
 127 sampling frequency varied among seasons and was reduced during the rainy  
 128 period, this dataset does not represent a uniformly sampled annual climatology.  
 129 Accordingly, the results are interpreted as observation-based estimates for the  
 130 sampled annual cycle, and caution is needed when extending them to annual-  
 131 scale representativeness. Precipitation and solar radiation data were obtained  
 132 from historical reanalysis products provided by the European Centre for  
 133 Medium-Range Weather Forecasts (ECMWF). All samples and field blanks  
 134 were stored in the dark at  $-20\text{ }^{\circ}\text{C}$  until analysis. This storage procedure helps  
 135 minimize post-collection changes, but it does not eliminate artifacts generated  
 136 during sampling itself. A summary of TSP mass concentrations, chemical  
 137 components, and meteorological conditions is provided in Table S1  
 138 (*Supplement*).



139

140 **Figure 1.** (a) Sampling site location in Bangkok, Thailand. (b) Classified air-mass  
141 trajectories (detailed in Figures S1 and S2). (c) Distribution of  $R_{land}$ , with samples  
142 categorized as marine-influenced ( $R_{land} < 0.3$ ), mixed-influenced ( $0.3 \leq R_{land} \leq 0.7$ ), or  
143 continental-influenced ( $R_{land} > 0.7$ ) based on  $R_{land}$  values. The map in panel (a) was created  
144 using ArcGIS software with the ESRI National Geographic World Map as the basemap.  
145 Sources: Esri, National Geographic, and its data providers; powered by Esri.

## 146 **2.2. Chemical Analysis**

147 Organic carbon (OC) and elemental carbon (EC) mass concentrations  
148 were determined using an OC/EC analyzer following the NIOSH 870 thermal-  
149 optical protocol. Inorganic ions ( $Cl^-$ ,  $NO_3^-$ ,  $SO_4^{2-}$ ,  $Na^+$ ,  $K^+$ ,  $NH_4^+$ ,  $Mg^{2+}$ , and  $Ca^{2+}$ )  
150 were quantified by ion chromatography (761 Compact IC, Metrohm,  
151 Switzerland), and trace elements were analyzed via inductively coupled  
152 plasma–mass spectrometry (ICP–MS; ELAN DRC II, PerkinElmer Ltd., Hong  
153 Kong). Analytical errors were 5.5% for OC, and 3.9% for EC, below 5.0% for  
154 trace elements, and under 1.0% for water-soluble ions, based on prior  
155 validation (Wang et al., 2020).

156 Polar molecular tracers—including BB markers (levoglucosan, mannosan,  
157 galactosan) and biogenic/anthropogenic secondary organic aerosol (SOA)  
158 tracers such as 2-methylglyceric acid (2-MGA), 2-methylthreitol and 2-  
159 methylerythritol (2-MGL), 3-methyl-1,2,3-butanetricarboxylic acid (MBTCA),  
160 and *o/p*-phthalic acid—were analyzed by gas chromatography–mass  
161 spectrometry (GC–MS) following derivatization as previously reported (Geng et  
162 al., 2020; Li et al., 2013). The mean recovery of  $^{13}C$ -labeled levoglucosan was  
163  $87\% \pm 10\%$ . Non-polar tracers of coal and fossil-fuel combustion (hopanes and  
164 steranes) were also analyzed, with perdeuterated tetracosane yielding a  
165 recovery of  $114\% \pm 11\%$  (Wang et al., 2020).

166 Water-soluble OC (WSOC) and water-soluble total nitrogen (WSTN) were  
167 extracted by ultrasonication for 30 minutes using ultrapure water (resistivity  $>$   
168  $18.2 M\Omega cm$ ), followed by filtration through  $0.22 \mu m$  PTFE membranes.  
169 Concentrations were measured with a TOC/TN analyzer (model TOC-Vcsh,  
170 Shimadzu). WSON was calculated as the difference between WSTN and water-  
171 soluble inorganic nitrogen (WSIN), where WSIN comprises  $NH_4^+$ -N,  $NO_3^-$ -N,  
172 and  $NO_2^-$ -N:  $[WSON] = [WSTN] - [WSIN]$ . Nitrite concentrations were  
173 consistently below the detection limit of ion chromatography and were excluded

174 from further analysis. It should be noted that some dissolved ON species may  
175 not be fully converted to nitrogen monoxide in the TOC/TN analyzer, potentially  
176 leading to underestimation of WSON (Miyazaki et al., 2011). Furthermore,  
177 integrated filter sampling may be affected by gas–particle sampling artifacts,  
178 including volatilization losses of semi-volatile inorganic nitrogen species and  
179 possible adsorption of gaseous nitrogen compounds on the filter. Previous  
180 studies suggested that adsorption of gaseous organics onto quartz filters may  
181 have only a limited effect on WSON measurement under similar sampling  
182 conditions, whereas volatilization loss during sampling may still lead to  
183 underestimation of particulate WSON (Matsumoto et al., 2014; Matsumoto and  
184 Yamato, 2016).

185 The relative standard deviation (RSD) for WSTN analysis was 3.6%  
186 (method) and 0.77% (instrument). Method detection limits were  $0.09 \mu\text{g m}^{-3}$  for  
187 WSON,  $0.03 \mu\text{g m}^{-3}$  for  $\text{NO}_3^-$ -N, and  $0.02 \mu\text{g m}^{-3}$  for  $\text{NH}_4^+$ -N. Field blank levels  
188 were  $0.067 \mu\text{gN m}^{-3}$  (WSON),  $0.043 \mu\text{gN m}^{-3}$  ( $\text{NH}_4^+$ -N), and  $0.07 \mu\text{gN m}^{-3}$   
189 ( $\text{NO}_3^-$ -N), corresponding to average blank-to-sample ratios of 7.1%, 4.3%, and  
190 12%, respectively, consistent with previous reports (Matsumoto et al., 2019a).  
191 All reported WSON and WSTN concentrations were blank-corrected and  
192 should be interpreted as operationally defined particulate water-soluble N  
193 concentrations under the applied sampling protocol.

### 194 **2.3. Source Apportionment**

195 The U.S. Environmental Protection Agency’s PMF model (PMF 5.0) was  
196 employed to perform factor analysis on environmental data with non-negativity  
197 constraints and to estimate associated uncertainties (Norris et al., 2014). PMF  
198 has been widely applied as a robust tool for aerosol source apportionment. In  
199 PMF 5.0, species are evaluated based on the signal-to-noise (S/N) ratio and  
200 can be classified as “strong,” “weak,” or “bad”. Weak species are retained but  
201 assigned a tripled uncertainty, whereas bad species are excluded from the  
202 modeling. In this study, WSON was included as a total variable to resolve its  
203 sources. Following the base run, rotational stability ( $F_{\text{peak}}$ ) tests were conducted,  
204 and model robustness was evaluated using the base model displacement  
205 (DISP), bootstrap (BS), and bootstrap displacement (BS-DISP) methods. A  
206 detailed description of PMF procedures is provided in Text S1 in *Supplement*.

## 207 2.4. Air Mass Back Trajectories and Trajectory-Based Chl-a Exposure

208 To identify potential source regions, we calculated 120-hour back  
209 trajectories using the Hybrid Single-particle Lagrangian Integrated Trajectory  
210 (HYSPLIT) model (<http://www.arl.noaa.gov/HYSPLIT.php>), driven by the Global  
211 Data Assimilation System (GDAS) meteorological dataset at  $1^\circ \times 1^\circ$  resolution  
212 (<http://ready.arl.noaa.gov/archives.php>). Trajectories were generated at 1-hour  
213 intervals and subsequently classified through cluster analysis (Figure 1b and  
214 Figures S1–S2). Based on origin and transport pathways, air masses arriving  
215 in Bangkok were grouped into six distinct clusters. During the Dry I season, air  
216 masses originated predominantly over the Gulf of Thailand/South China Sea  
217 (clusters 1–2), with a minor contribution from the Indochina Peninsula (cluster  
218 3). In the Wet season, trajectories were primarily transported via the South  
219 China Sea/Gulf of Thailand and the Arabian Sea (clusters 1, 2, 6), whereas Dry  
220 II season air masses mainly originated over mainland China and crossed the  
221 Indochina Peninsula (clusters 3–5).

222 Furthermore, the air mass retention ratio over land ( $R_{land}$ ), defined as the  
223 weighted ratio of transport time over land to the total transport duration, was  
224 calculated according to the method of Zhou et al. (2021, 2023) using Equation  
225 1. This parameter provides a quantitative measure of terrestrial influence at the  
226 receptor site. A schematic illustration is presented in Figure S3.

$$227 R_{land} = \frac{\sum_{i=1}^{N_{land}} e^{-t_i/120}}{\sum_{i=1}^{N_{total}} e^{-t_i/120}} \quad (1)$$

228 Here,  $N_{total}$  denotes the total number of trajectory endpoints and  $N_{land}$   
229 the number over land. The backward tracking time  $t_i$  (in hours) and the  
230 weighting factor  $e^{-t_i/120}$  account for the diminishing influence of distant  
231 regions due to air mass diffusion and particle deposition during transport. As a  
232 result, regions associated with longer backward tracking times exert a weaker  
233 influence on the receptor site compared to nearby areas. Based on the  $R_{land}$   
234 values (Figure 1c), samples were categorized as marine-influenced ( $R_{land} < 0.3$ ),  
235 mixed-influenced ( $0.3 \leq R_{land} \leq 0.7$ ), or continental-influenced ( $R_{land} > 0.7$ ). It  
236 should be noted that marine-influenced air masses, as defined by low  $R_{land}$ , do  
237 not necessarily represent purely marine-biogenic conditions, because aged  
238 marine aerosol, shipping emissions, and anthropogenically polluted air masses  
239 transported over the ocean may also contribute to aerosol composition. This

240 classification is further supported by molecular marker analysis: during marine-  
 241 influenced periods, the regression slope for Na<sup>+</sup> versus Mg<sup>2+</sup> (0.11) closely  
 242 aligned with the seawater reference ratio (0.12). Elevated levels of Cl<sup>-</sup>, Na<sup>+</sup>,  
 243 Mg<sup>2+</sup>, and the Na<sup>+</sup>/Σions ratio consistently reflected enhanced sea-salt  
 244 influence during marine-influenced periods. By contrast, non-sea-salt sulfate  
 245 (nss-SO<sub>4</sub><sup>2-</sup>) was not interpreted here as a unique indicator of marine origin,  
 246 because it may include contributions from both anthropogenic sulfur and marine  
 247 biogenic sulfur and may also reflect secondary atmospheric processing during  
 248 transport (Savoie et al., 2002). Particulate NO<sub>3</sub><sup>-</sup> was mainly interpreted as a  
 249 secondary product formed from the oxidation of NO<sub>x</sub> emitted by combustion-  
 250 related sources, including traffic, shipping, industrial activities, and fossil-fuel  
 251 combustion or BB, followed by gas-to-particle partitioning or heterogeneous  
 252 reactions with sea-salt particles during transport (Pryor and Sørensen, 2000).  
 253 Its concentration was lowest during marine-influenced periods, lower than  
 254 under mixed- and continental-influenced conditions, a pattern consistent with  
 255 combustion-derived species such as non-sea-salt K<sup>+</sup> (nss-K<sup>+</sup>), EC, and  
 256 levoglucosan. These results indicate reduced, but not absent, terrestrial and  
 257 anthropogenic influence during marine-influenced periods (Table S2).

258 Air mass exposure to Chl-a (AEC), defined as the mean sea surface Chl-a  
 259 concentration along air mass trajectories, was used as a proxy for marine  
 260 biogenic emissions at the receptor site (Park et al., 2018; Zhou et al., 2023). A  
 261 statistically significant positive correlation was observed when air masses  
 262 traveled within the marine boundary layer. However, due to the relatively low  
 263 correlation between AEC and methanesulfonate, the formulation was adjusted  
 264 based on the approach of Zhou et al. (2021, 2023), as follows:

$$265 \quad AEC = \frac{\sum_{i=1}^{N_{total}} Chl-a_i \cdot e^{-t_i/120} \cdot e^{-h_i/500}}{n} \quad (2)$$

266 Here,  $N_{total}$  denotes the total number of hourly endpoints (120, including  
 267 the receptor point) along the trajectory. The variable  $Chl-a_i$  represents the  
 268 mean Chl-a concentration—derived from MODIS-Aqua monthly composites at  
 269 a 4 km resolution—within a 20 km radius of the  $i_{th}$  trajectory endpoint. Endpoints  
 270 over land were assigned  $Chl-a_i =$  zero. The weighting factor  $e^{-h_i/500}$   
 271 accounts for the influence of altitude  $h_i$ , reflecting the reduced contribution from  
 272 higher altitudes due to Chl-a dilution and particle deposition during transport.  
 273 The denominator  $n$  corresponds to the number of trajectory endpoints with

274 valid Chl-a data, including zero values over land.

## 275 **2.5. Potential Source Contribution Function (PSCF) Model**

276 The PSCF model was employed to identify source regions by discretizing  
277 the study domain into an  $i \times j$  grid. The PSCF values, ranging from 0 to 1,  
278 represent the conditional probability that an air parcel passing through a grid  
279 cell contributes to high concentrations at the receptor site; elevated values  
280 denote a higher probability of source contribution. In this study, PSCF analysis  
281 was applied to identify potential geographic source regions of both total WSON  
282 and PMF-resolved source categories of WSON in aerosols collected in  
283 Bangkok. A detailed description of the PSCF methodology is provided in Text  
284 S2 and in previous publications (Geng et al., 2020; Tang et al., 2024).

## 285 **3. Results and Discussion**

### 286 **3.1. Temporal Variations of WSON**

287 Figure S4 and Table S1 present the temporal variations and statistical  
288 summaries of meteorological parameters and chemical compositions in TSP  
289 throughout the sampling campaign. In Bangkok, Thailand, the mass  
290 concentrations of TSP, OC, and EC were  $55 \pm 30 \mu\text{g m}^{-3}$  ( $17\text{--}161 \mu\text{g m}^{-3}$ ),  $12$   
291  $\pm 6.3 \mu\text{g m}^{-3}$  ( $3.7\text{--}38 \mu\text{g m}^{-3}$ ), and  $1.4 \pm 0.43 \mu\text{g m}^{-3}$  ( $0.16\text{--}2.8 \mu\text{g m}^{-3}$ ),  
292 respectively. The TSP levels in this region were substantially lower than those  
293 reported in other areas, such as the Eastern Mediterranean ( $220 \pm 105 \mu\text{g m}^{-3}$ ;  
294 Tripathee et al., 2021), Jiaozhou Bay ( $134 \pm 80 \mu\text{g m}^{-3}$ ; Xing et al., 2018), and  
295 Xi'an during the dust episodes ( $2109 \pm 1360 \mu\text{g m}^{-3}$ ; Wang et al., 2014).  
296 Pronounced seasonal variations were observed: TSP levels decreased by 56%  
297 from the Dry I season to the Wet season, but increased by 52% during the Dry  
298 II season. In Bangkok, rainfall during the Wet season (April to October)  
299 accounted for 92% of the annual precipitation total. To examine wet scavenging  
300 effects, we evaluated the relationship between TSP concentrations and  
301 precipitation (Figure S5a). A significant negative correlation was identified ( $R^2$   
302  $= 0.22$ ,  $p < 0.001$ ), consistent with a contribution from wet scavenging, although  
303 the relatively low explanatory power indicates that emissions, transport, and  
304 precipitation history along the air-mass pathway also substantially influenced  
305 TSP variability.

306 The mass fraction of WSTN in TSP collected in Bangkok averaged  $3.8\% \pm$   
307  $1.1\%$  ( $2.2\%\text{--}7.2\%$ ), which was somewhat higher than that reported in the

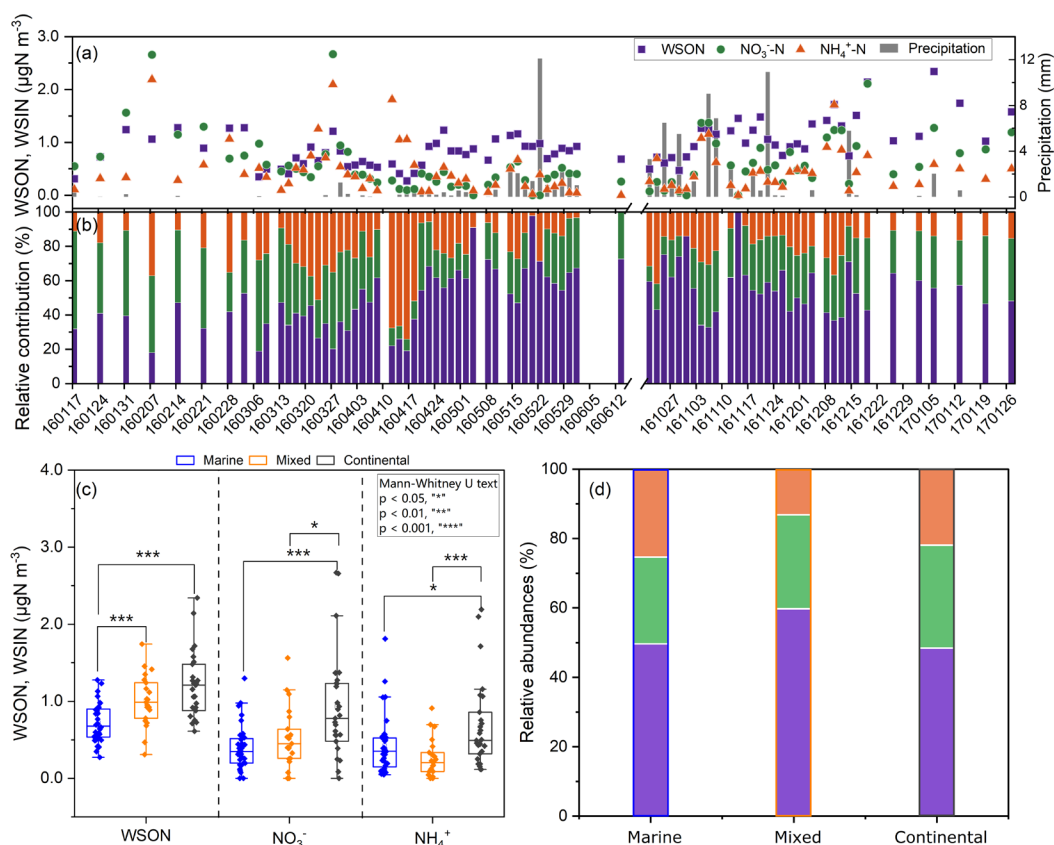
308 Eastern Mediterranean (~2.7%; Tripathee et al., 2021) and comparable to  
309 values from Sapporo, Japan ( $3.8\% \pm 2.3\%$ ; Pavuluri et al., 2015). As shown in  
310 Figure 2a and Table S2, the concentrations of the individual WSTN components,  
311 including WSON,  $\text{NO}_3^-$ -N, and  $\text{NH}_4^+$ -N, were  $0.95 \pm 0.40 \mu\text{gN m}^{-3}$  ( $0.27$ – $2.3$   
312  $\mu\text{gN m}^{-3}$ ),  $0.60 \pm 0.52 \mu\text{gN m}^{-3}$  (below detection limitation (BDL)– $2.7 \mu\text{gN m}^{-3}$ ),  
313 and  $0.47 \pm 0.44 \mu\text{gN m}^{-3}$  (BDL– $2.2 \mu\text{gN m}^{-3}$ ), respectively. WSON correlated  
314 positively with both TSP ( $r = 0.65$ ,  $p < 0.01$ ) and WSIN ( $r = 0.51$ ,  $p < 0.01$ )  
315 (Figure S6), indicating that WSON variability was linked to overall aerosol  
316 loading and co-varied with inorganic N across the dataset.

317 Concentrations of WSON,  $\text{NO}_3^-$ -N,  $\text{NH}_4^+$ -N, TSP, OC, and EC varied  
318 considerably under different air mass regimes (Table S2). The nonparametric  
319 Mann–Whitney U test indicated that WSON and  $\text{NO}_3^-$ -N levels were  
320 significantly lower during marine-influenced periods than under mixed or  
321 continental conditions (Figure 2c,  $p < 0.001$ ). In contrast,  $\text{NH}_4^+$ -N concentrations  
322 were slightly higher during marine periods. This contrast indicates that the  
323 responses of individual N species were not uniform across air-mass regimes  
324 and should not be attributed to a single dominant source. This aligns with earlier  
325 studies reporting that aerosols in remote marine regions may still be  
326 substantially influenced by continental inputs (Jickells et al., 2013). BB tracers  
327 (e.g., levoglucosan, galactosan, mannosan) were also significantly lower during  
328 marine-influenced days (see Table S2). Furthermore, WSON correlated with BB  
329 and SOA markers and aerosol liquid water content (ALWC, Text S3) under  
330 mixed and continental conditions, whereas these associations were not evident  
331 during marine periods (Figure S7). Taken together, these patterns suggest that  
332 the lower WSON concentrations during marine-influenced periods likely  
333 reflected a combination of reduced continental and combustion-related  
334 influence, differences in transport history, and atmospheric processing.  
335 Seasonally higher rainfall may also have contributed, but because no significant  
336 direct correlation was found between WSON and precipitation (Figure S5b),  
337 precipitation alone cannot explain the observed WSON variability.

338 The WSON/WSTN ratio during marine-influenced days ( $50\% \pm 17\%$ ) was  
339 similar to that under continental influence ( $48\% \pm 15\%$ ) but lower than during  
340 mixed conditions ( $60\% \pm 17\%$ ) (Figure 2d). This pattern shows that the  
341 WSON/WSTN ratio alone may not be a reliable way to identify WSON source  
342 in this dataset. The elevated ratio under mixed conditions likely reflects

343 overlapping marine and continental influences together with different responses  
344 of WSON and WSIN to transport and removal processes, rather than a unique  
345 source type. During marine-influenced periods, WSON may reflect both marine-  
346 related contributions and anthropogenic inputs associated with shipping  
347 emissions and atmospheric processing, whereas continental periods are more  
348 strongly affected by terrestrial anthropogenic emissions. Precipitation may alter  
349 the WSON/WSTN ratio through differential scavenging: WSIN species (e.g.,  
350  $\text{NO}_3^-$ ,  $\text{NH}_4^+$ ) are efficiently removed by rainfall (Matsumoto et al., 2019b; Nehir  
351 and Koçak, 2018), as WSIN showed stronger correlations with precipitation  
352 (Figure S5c,d). By contrast, the absence of a significant WSON–precipitation  
353 correlation indicates that WSON variability in this dataset was less directly  
354 coupled to precipitation, rather than supporting a distinct scavenging  
355 mechanism.

356       Annually, WSON accounted for  $52\% \pm 17\%$  of the WSTN (Figure 2b)—  
357 substantially higher than values reported from a forest site ( $20\% \pm 11\%$ ;  
358 Miyazaki et al., 2014), an offshore island ( $27\%$ ; Tian et al., 2023), Sapporo ( $9.2\%$   
359  $\pm 7.3\%$ ; Pavuluri et al., 2015), and coastal Qingdao ( $\sim 20\%$ ; Shi et al., 2010).  
360 Elevated WSON/WSTN ratios have been documented in source emissions  
361 such as BB ( $80\% \pm 6.3\%$ ), vehicle exhaust ( $67\% \pm 16\%$ ), and shipping  
362 emissions ( $54\% \pm 31\%$ ) (Yu et al., 2017), as well as receptor regions such as  
363 Hawaii ( $64\%$ ; Cornell et al., 2001) and polluted continental urban regions such  
364 as Xi'an ( $45\%$ , range:  $22\%$ – $68\%$ ; Ho et al., 2015). By comparison, the South  
365 China Sea, which is more strongly influenced by open-marine conditions,  
366 exhibited a WSON/WSTN ratio of  $34\%$ , whereas the Yellow Sea, subject to  
367 stronger continental and anthropogenic influence, showed a lower ratio of  $17\%$   
368 (Shi et al., 2010). During phytoplankton blooms, ON can dominate aerosol  
369 composition, contributing up to  $84\%$  of WSTN (Violaki et al., 2015) and  $63\%$  of  
370 submicrometer aerosol mass (O'Dowd et al., 2004). Collectively, these studies  
371 indicate that elevated WSON/WSTN ratios may arise from anthropogenic  
372 combustion sources, shipping emissions, marine-related emissions, and  
373 secondary atmospheric processing. Therefore, the WSON/WSTN ratio alone is  
374 insufficient to discriminate marine-biogenic, shipping-related, and continental  
375 anthropogenic sources of WSON. More quantitative approaches are needed to  
376 apportion the origins of aerosol ON.  
377



378

379 **Figure 2.** Temporal variations and source influences on N species in Bangkok aerosols.

380 (a) Time-series of concentrations of WSON and WSIN ( $\text{NH}_4^+\text{-N}$ ,  $\text{NO}_3^-\text{-N}$ ), overlaid with

381 daily rainfall from ECMWF reanalysis data. (b) Relative contributions of WSON and WSIN

382 to WSTN across the study period. (c) Concentration distributions and (d) relative

383 abundances of WSON and WSIN during marine-, mixed-, and continental-influenced

384 periods.

### 385 3.2. SSA as a Major WSON Source in Marine-influenced Days

386 To elucidate the contributions of marine and anthropogenic sources to

387 WSON in this coastal urban environment, we applied the PMF 5.0 model to 84

388 aerosol samples characterized by 26 chemical species. The model resolved

389 WSON into seven source factors: shipping emissions, secondary sulfate, dust,

390 SOA, BB, vehicle emissions and fossil-fuel combustion (VEFC), and SSA

391 (Figure S8); the detailed identification of each factor is provided in Text S1. The

392 SSA factor was characterized primarily by high loadings of  $\text{Na}^+$ ,  $\text{Cl}^-$ , and  $\text{Mg}^{2+}$ ,

393 with WSON also contributing to this factor. We therefore interpret this factor as

394 a sea-salt-associated aerosol carrying WSON, rather than as purely biogenic

395 aerosol. Furthermore, PSCF mapping of SSA-associated WSON pointed

396 mainly to the Gulf of Thailand and, to a lesser extent, the Bay of Bengal (see  
397 Figure S10), supporting the importance of marine-related source regions for  
398 this factor.

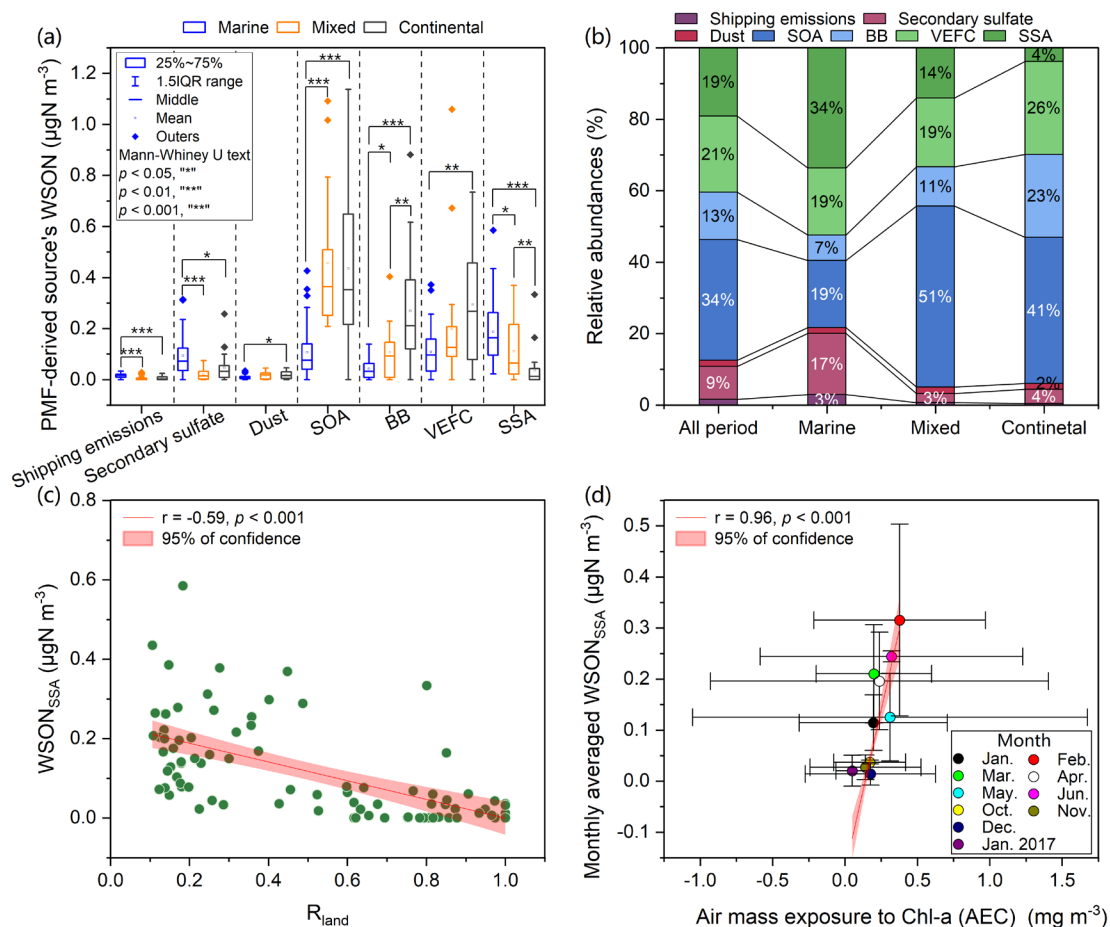
399 Over the entire study period, SOA ( $34\% \pm 25\%$ ), VEFC ( $21\% \pm 16\%$ ), SSA  
400 ( $19\% \pm 19\%$ ), and BB ( $13\% \pm 12\%$ ) emerged as the dominant sources of WSON  
401 in Bangkok aerosols (Figures 3b and S9). This is consistent with previous  
402 reports highlighting secondary formation and BB as major contributors to  
403 WSON (Leung et al., 2024; Tsagkaraki et al., 2021; Yu et al., 2017). Earlier  
404 factor-based studies also indicated that sea salt can explain over 20% of the  
405 variance in WSON (Chen and Chen, 2010; Shi et al., 2010). The contribution  
406 of SSA in our study, however, exceeded values reported for other coastal  
407 regions such as Hong Kong (4.4%) and the Eastern Mediterranean ( $<5\%$ )  
408 (Leung et al., 2024; Nehir and Koçak, 2018; Tsagkaraki et al., 2021). Two  
409 factors may explain this discrepancy. First, ON in coarse aerosols often  
410 originates from soil, dust, or large sea-salt particles (Cornell et al., 2001; Mace  
411 et al., 2003), whereas studies focusing on  $PM_{2.5}$ —such as those in Hong  
412 Kong—naturally record lower sea-salt contributions (Leung et al., 2024).  
413 Second, the ultra-oligotrophic marine environment of the Eastern  
414 Mediterranean, characterized by low nutrient availability and limited riverine  
415 input, results in low marine productivity and thus diminished marine-derived  
416 WSON (Nehir and Koçak, 2018; Tsagkaraki et al., 2021).

417 We further disaggregated WSON source contributions by air mass regime  
418 (Figure 3b). Under marine influence, SSA constituted the dominant source of  
419 WSON ( $34\% \pm 17\%$ ), exceeding SOA ( $19\% \pm 17\%$ ), VEFC ( $19\% \pm 14\%$ ), and  
420 secondary sulfate ( $17\% \pm 16\%$ ), while BB contributed minimally ( $7.1\% \pm 6.0\%$ ).  
421 This pattern is consistent with studies conducted in remote marine and island  
422 settings (Altieri et al., 2016; Miyazaki et al., 2011; Violaki et al., 2015). Under  
423 mixed marine–continental influence, SOA became the dominant contributor ( $51\%$   
424  $\pm 20\%$ ), followed by VEFC ( $19\% \pm 14\%$ ) and SSA ( $14\% \pm 15\%$ ). During  
425 continental conditions, SOA remained the primary source ( $41\% \pm 26\%$ ), likely  
426 reflecting multiple secondary formation pathways of nitrogen-containing organic  
427 aerosol, of which nitroaromatics may represent one possible subset of these  
428 compounds (Xie et al., 2017). Previous work has shown that oxidized  $\alpha$ -pinene  
429 SOA can account for 33%–38% of WSON, with aerosol liquid water further  
430 promoting nighttime secondary WSON formation (Xu et al., 2020). Under

431 continental regimes, VEFC ( $26\% \pm 19\%$ ) and BB ( $23\% \pm 14\%$ ) also contributed  
432 substantially to WSON. Notably, the SSA contribution dropped sharply to  $3.8\%$   
433  $\pm 6.4\%$  under continental influence. Expressed relative to total WSTN, SSA-  
434 associated WSON contributed approximately  $1.6\% \pm 2.1\%$ ,  $7.3\% \pm 7.6\%$ , and  
435  $13\% \pm 8.2\%$  under continental-, mixed-, and marine-influenced conditions,  
436 respectively, with an overall mean contribution of  $7.8\% \pm 8.2\%$  over the sampled  
437 annual cycle, further illustrating its enhanced importance during marine  
438 influence.

439 Temporal variations in source-resolved WSON concentrations are shown  
440 in Figure 3a. Among the three air mass regimes, SSA-associated WSON  
441 concentrations peaked under marine influence ( $0.19 \pm 0.12 \mu\text{gN m}^{-3}$ ),  
442 approximately 1.7 times higher than during mixed periods ( $0.11 \pm 0.12 \mu\text{gN m}^{-3}$ )  
443 and five times higher than during continental periods ( $0.037 \pm 0.069 \mu\text{gN m}^{-3}$ ).  
444 Shipping-emission-associated WSON was also elevated during marine days  
445 ( $0.015 \pm 0.0075 \mu\text{gN m}^{-3}$ ) relative to mixed and continental periods, though its  
446 overall contribution remained low ( $\sim 3\%$ ). WSON associated with the secondary  
447 sulfate factor under marine influence ( $0.094 \pm 0.086 \mu\text{gN m}^{-3}$ ) was significantly  
448 higher than during mixed periods ( $0.022 \pm 0.023 \mu\text{gN m}^{-3}$ ) and during  
449 continental periods ( $0.046 \pm 0.056 \mu\text{gN m}^{-3}$ ), consistent with an important  
450 contribution from secondary inorganic aerosol formation. Although the PMF-  
451 resolved shipping factor remained low during marine-influenced periods, other  
452 anthropogenic-related factors, including secondary sulfate, VEFC and SOA,  
453 still showed non-negligible contributions, consistent with the view that marine-  
454 influenced air masses in this study should not be interpreted as purely marine-  
455 biogenic conditions. These results also indicate that marine air mass transport  
456 plays an important role in the enhancement of SSA-associated WSON, further  
457 supported by a strong negative correlation between SSA-associated WSON  
458 and  $R_{\text{land}}$  (Figure 3c,  $r = -0.59$ ,  $p < 0.001$ ). In contrast, SOA-, BB-, and VEFC-  
459 associated WSON increased significantly under mixed and continental  
460 conditions. Although SOA is generally considered more susceptible to wet  
461 removal than primary aerosol (Sun et al., 2011; Zhao et al., 2026), no significant  
462 correlation was observed between precipitation and PMF-resolved source  
463 concentrations in this dataset. This suggests that wet scavenging alone did not  
464 dominate the observed source-resolved WSON variability.

465



466

467

**Figure 3.** Source apportionment of WSON based on PMF. (a) Absolute concentrations and

468

(b) relative contributions of PMF-resolved sources to total WSON during the entire study

469

period and under marine-, mixed-, and continental-influenced conditions. (c) Correlation

470

between  $R_{\text{land}}$  and SSA-associated WSON. (d) Relationship between AEC and monthly

471

averaged SSA-associated WSON concentrations, color-coded by sampling month.

472

### 3.3. Marine Productivity as a Key Factor Influencing Coastal WSON

473

#### Distribution

474

SSA is dominated by inorganic sea salt but can also comprise an important

475

organic fraction derived from ocean-surface materials (Prather et al., 2013;

476

Quinn et al., 2014; Schiffer et al., 2018). Previous studies have linked marine

477

biological productivity to the organic enrichment of SSA (O'Dowd et al., 2015;

478

Violaki et al., 2015), and Chl-a has often been used as a broad proxy for ocean-

479

surface biological conditions (Facchini et al., 2008; O'Dowd et al., 2004). Given

480

the substantial contribution of SSA-associated WSON to total WSON and

481

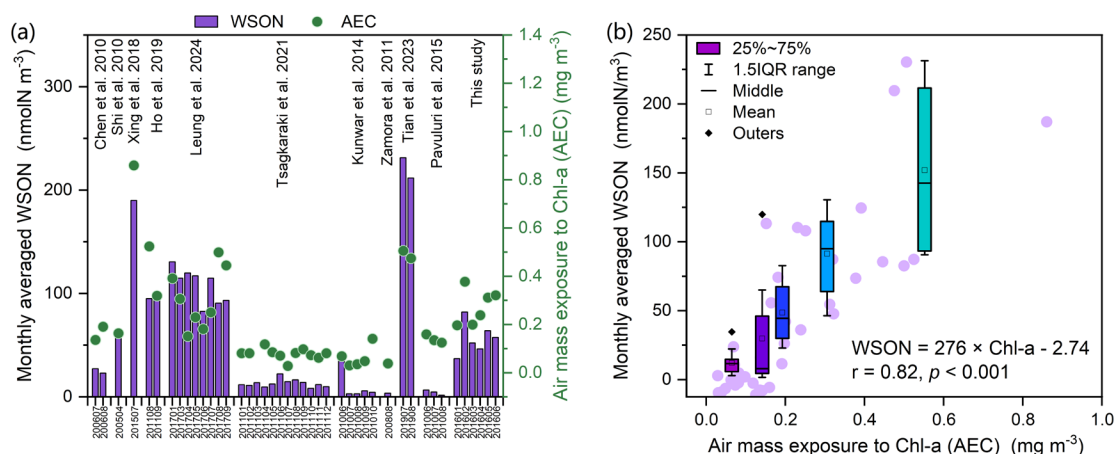
WSTN during marine-influenced periods in our study, we further examined

482

whether marine productivity was related to its variability.

483 We calculated AEC values based on monthly MODIS Chl-a data (4 km  
484 resolution) along 120-hour backward trajectories (see Methods). SSA-  
485 associated WSON exhibited a strong positive correlation with AEC ( $r = 0.96$ ,  $p$   
486  $< 0.001$ ; Figure 3d), consistent with a linkage between marine productivity and  
487 the variability of this factor. This contrasts with Tian et al. (2023), who observed  
488 significant WSON-AEC correlations only in summer, likely reflecting stronger  
489 anthropogenic influences and/or weaker marine signals during other seasons.  
490 While previous multivariate regression identified wind speed and Chl-a as key  
491 predictors of the organic fraction in SSA (Gantt et al., 2011), other studies note  
492 that Chl-a alone may not fully capture organic enrichment (Rinaldi et al., 2013).  
493 Still, moderate correlations ( $r \approx 0.60$ ) between Chl-a and marine organic aerosol  
494 abundance have been reported (Sciare et al., 2009). However, AEC may also  
495 covary with marine transport conditions, meteorology, and other seasonally  
496 structured processes, and correlation alone does not establish source  
497 dominance. Taken together, the PMF results, reduced terrestrial influence, and  
498 the positive AEC relationship are consistent with an important marine-biogenic  
499 enhancement of SSA-associated WSON during marine-influenced periods,  
500 although shipping and other anthropogenic co-influences cannot be fully  
501 excluded.

502 To further examine the broader relevance of this relationship, we compiled  
503 a dataset of WSON concentrations from coastal and island sites and  
504 recalculated air-mass trajectories,  $R_{\text{land}}$ , and AEC values based on MODIS Chl-  
505 a for each site (Figure 4a and Table S3). Across these marine-influenced  
506 coastal datasets, the highest WSON concentrations occurred at Huaniao Island  
507 (Tian et al., 2023), followed by Jiaozhou Bay (Xing et al., 2018), Hong Kong (Ho  
508 et al., 2019; Leung et al., 2024), the South China Sea (Shi et al., 2010), and  
509 Bangkok. The lowest values were observed in the Eastern Mediterranean  
510 (Tsagkaraki et al., 2021), Keelung City (Chen and Chen, 2010), Okinawa Island  
511 (Kunwar and Kawamura, 2014), Barbados (Zamora et al., 2011), and Sapporo  
512 (Pavuluri et al., 2015). Notably, spatial patterns in AEC closely mirrored those  
513 in WSON. A significant positive correlation was found between WSON and AEC  
514 across all sites ( $r = 0.82$ ,  $\text{WSON} [\text{nmol m}^{-3}] = 276 \times \text{AEC} [\text{mg m}^{-3}] - 2.74$ ,  
515 Figure 4b). This large-scale comparison supports the broader consistency of  
516 the observed relationship, although the influence of site-to-site differences in  
517 sampling protocol, aerosol size fraction, and anthropogenic impact cannot be  
518 excluded.



519

520 **Figure 4.** (a) Geographic distributions and (b) correlation between AEC values and monthly  
 521 mean WSON concentration in coastal regions predominantly influenced by marine air  
 522 masses. Values are provided in Table S3. Air mass trajectories for these coastal and island  
 523 sampling sites were recalculated using the HYSPLIT model, and AEC values were derived  
 524 from MODIS monthly Chl-a concentrations.

525

#### 4. Conclusions

526

527 The equation derived in this study ( $WSON [nmol m^{-3}] = 276 \times AEC [mg$   
 528  $m^{-3}] - 2.74$ ) provides an empirical basis for examining the linkage between  
 529 coastal aerosol water-soluble organic nitrogen (WSON) and oceanic biological  
 530 conditions along air-mass transport pathways. Our results indicate that sea  
 531 spray aerosol (SSA)-associated WSON is an important contributor to coastal  
 532 aerosol WSON under marine-influenced conditions, and its covariation with  
 533 trajectory-based air-mass exposure to chlorophyll-a (Chl-a) (AEC) is consistent  
 534 with marine-biogenic enhancement. However, these implications should be  
 535 interpreted with caution because the present dataset was obtained with  
 536 seasonally uneven sampling coverage, 24 h integrated filter sampling, and  
 537 without isotopic constraints that could more directly distinguish marine-biogenic,  
 538 shipping-related, and continental anthropogenic sources. Future work  
 539 combining more temporally uniform observations with isotopic and molecular-  
 540 level characterization is needed to further strengthen source attribution. We  
 541 therefore suggest that integrating satellite-derived Chl-a data into air mass  
 542 trajectory analyses may help improve future assessments of marine-related  
 WSON variability.

543

#### Code and data availability.

544

The analysis outputs and code used in this study are publicly available from

545 the Open Science Framework (OSF) repository at  
546 <https://doi.org/10.17605/OSF.IO/YMJ3F> (Tang et al., 2026).

#### 547 **Supplement**

548 The supplement related to this article is available online.

#### 549 **Author contributions**

550 Conceptualization: JT. Funding acquisition: JT, SH, SZ, and GZ.  
551 Investigation: JT, XW, JW, SL, XG, GuZ, and SB. Methodology: JT, XW,  
552 and JW. Project administration: GZ and SZ. Resources: YM, SZ, JL, and  
553 GZ. Software: XW, and SL. Supervision: JL, SZ, and GZ. Validation: JT and  
554 SZ. Writing (original draft): JT. Writing (review and editing): XW, SH, SZ,  
555 and GZ.

#### 556 **Competing interests**

557 The authors declare no competing financial interest.

#### 558 **Acknowledgments**

559 This research has been supported by the National Natural Science  
560 Foundation of China (442192511 and 42473070), the Guangdong Basic and  
561 Applied Basic Research Foundation (2023B0303000007 and  
562 2023B1515020067), and the National Science Foundation of Chongqing  
563 (CSTB2024NSCQ-MSX0897).

#### 564 **References**

- 565 Altieri, K. E., Fawcett, S. E., Peters, A. J., Sigman, D. M., and Hastings, M. G.: Marine  
566 biogenic source of atmospheric organic nitrogen in the subtropical North Atlantic, *Proc.*  
567 *Natl. Acad. Sci. U. S. A.*, 113, 925-930, <https://doi.org/10.1073/pnas.1516847113>, 2016.
- 568 Altieri, K. E., Hastings, M. G., Peters, A. J., and Sigman, D. M.: Molecular characterization  
569 of water soluble organic nitrogen in marine rainwater by ultra-high resolution  
570 electrospray ionization mass spectrometry, *Atmos. Chem. Phys.*, 12, 3557-3571,  
571 <https://doi.org/10.5194/acp-12-3557-2012>, 2012.
- 572 Buchanan, P. J., Aumont, O., Bopp, L., Mahaffey, C., and Tagliabue, A.: Impact of  
573 intensifying nitrogen limitation on ocean net primary production is fingerprinted by  
574 nitrogen isotopes, *Nat. Commun.*, 12, 6214, <https://doi.org/10.1038/s41467-021-26552-w>, 2021.
- 576 Cape, J. N., Cornell, S. E., Jickells, T. D., and Nemitz, E.: Organic nitrogen in the  
577 atmosphere — Where does it come from? A review of sources and methods, *Atmos.*  
578 *Res.*, 102, 30-48, <https://doi.org/10.1016/j.atmosres.2011.07.009>, 2011.
- 579 Chen, H.-Y., and Chen, L.-D.: Occurrence of water soluble organic nitrogen in aerosols at  
580 a coastal area, *J. Atmos. Chem.*, 65, 49-71, <https://doi.org/10.1007/s10874-010-9181-y>,

581 2010.

582 Cornell, S., Mace, K., Coeppicus, S., Duce, R., Huebert, B., Jickells, T., and Zhuang, L. Z.:  
583 Organic nitrogen in Hawaiian rain and aerosol, *J. Geophys. Res.-Atmos.*, 106, 7973-  
584 7983, <https://doi.org/10.1029/2000jd900655>, 2001.

585 Facchini, M. C., Decesari, S., Rinaldi, M., Carbone, C., Finessi, E., Mircea, M., Fuzzi, S.,  
586 Moretti, F., Tagliavini, E., Ceburnis, D., and O'Dowd, C. D.: Important Source of Marine  
587 Secondary Organic Aerosol from Biogenic Amines, *Environ. Sci. Technol.*, 42, 9116-9121,  
588 <https://doi.org/10.1021/es8018385>, 2008.

589 Gantt, B., Meskhidze, N., Facchini, M. C., Rinaldi, M., Ceburnis, D., and O'Dowd, C. D.:  
590 Wind speed dependent size-resolved parameterization for the organic mass fraction of  
591 sea spray aerosol, *Atmos. Chem. Phys.*, 11, 8777-8790, <https://doi.org/10.5194/acp-11-8777-2011>, 2011.

593 Geng, X., Mo, Y., Li, J., Zhong, G., Tang, J., Jiang, H., Ding, X., Malik, R. N., and Zhang,  
594 G.: Source apportionment of water-soluble brown carbon in aerosols over the northern  
595 South China Sea: Influence from land outflow, SOA formation and marine emission,  
596 *Atmos. Environ.*, 229, 117484, <https://doi.org/10.1016/j.atmosenv.2020.117484>, 2020.

597 He, Q., Li, C., Siemens, K., Morales, A. C., Hettiyadura, A. P. S., Laskin, A., and Rudich,  
598 Y.: Optical Properties of Secondary Organic Aerosol Produced by Photooxidation of  
599 Naphthalene under NO<sub>x</sub> Condition, *Environ. Sci. Technol.*, 56, 4816-4827,  
600 <https://doi.org/10.1021/acs.est.1c07328>, 2022.

601 Ho, K. F., Ho, S. S. H., Huang, R.-J., Liu, S. X., Cao, J.-J., Zhang, T., Chuang, H.-C., Chan,  
602 C. S., Hu, D., and Tian, L.: Characteristics of water-soluble organic nitrogen in fine  
603 particulate matter in the continental area of China, *Atmos. Environ.*, 106, 252-261,  
604 <https://doi.org/10.1016/j.atmosenv.2015.02.010>, 2015.

605 Ho, S. S. H., Li, L., Qu, L., Cao, J., Lui, K. H., Niu, X., Lee, S.-C., and Ho, K. F.: Seasonal  
606 behavior of water-soluble organic nitrogen in fine particulate matter (PM<sub>2.5</sub>) at urban  
607 coastal environments in Hong Kong, *Air Qual. Atmos. Health*, 12, 389-399,  
608 <https://doi.org/10.1007/s11869-018-0654-5>, 2019.

609 Ito, A., Lin, G., and Penner, J. E.: Reconciling modeled and observed atmospheric  
610 deposition of soluble organic nitrogen at coastal locations, *Global Biogeochem. Cycles*,  
611 28, 617-630, <https://doi.org/10.1002/2013GB004721>, 2014.

612 Jickells, T., Baker, A. R., Cape, J. N., Cornell, S. E., and Nemitz, E.: The cycling of organic  
613 nitrogen through the atmosphere, *Philos. Trans. R. Soc. B-Biol. Sci.*, 368,  
614 <https://doi.org/10.1098/rstb.2013.0115>, 2013.

615 Kanakidou, M., Duce, R. A., Prospero, J. M., Baker, A. R., Benitez-Nelson, C., Dentener,  
616 F. J., Hunter, K. A., Liss, P. S., Mahowald, N., Okin, G. S., Sarin, M., Tsigaridis, K.,  
617 Uematsu, M., Zamora, L. M., and Zhu, T.: Atmospheric fluxes of organic N and P to the  
618 global ocean, *Global Biogeochem. Cycles*, 26, <https://doi.org/10.1029/2011gb004277>,  
619 2012.

620 Kunwar, B., and Kawamura, K.: One-year observations of carbonaceous and nitrogenous  
621 components and major ions in the aerosols from subtropical Okinawa Island, an outflow  
622 region of Asian dusts, *Atmos. Chem. Phys.*, 14, 1819-1836, <https://doi.org/10.5194/acp-14-1819-2014>, 2014.

623 14-1819-2014, 2014.

624 Leung, C. W., Wang, X., and Hu, D.: Characteristics and source apportionment of water-  
625 soluble organic nitrogen (WSO<sub>N</sub>) in PM<sub>2.5</sub> in Hong Kong: With focus on amines, urea,  
626 and nitroaromatic compounds, *J. Hazard. Mater.*, 469, 133899,  
627 <https://doi.org/10.1016/j.jhazmat.2024.133899>, 2024.

628 Li, J. J., Wang, G. H., Cao, J. J., Wang, X. M., and Zhang, R. J.: Observation of biogenic  
629 secondary organic aerosols in the atmosphere of a mountain site in central China:  
630 temperature and relative humidity effects, *Atmos. Chem. Phys.*, 13, 11535-11549,  
631 <https://doi.org/10.5194/acp-13-11535-2013>, 2013.

632 Li, R., Cui, L., Zhao, Y., Fu, H., Li, Q., Zhang, L., and Chen, J.: Size-segregated water-  
633 soluble N-bearing species in the land-sea boundary zone of East China, *Atmos. Environ.*,  
634 218, 116990, <https://doi.org/10.1016/j.atmosenv.2019.116990>, 2019.

635 Li, Y., Fu, T.-M., Yu, J. Z., Yu, X., Chen, Q., Miao, R., Zhou, Y., Zhang, A., Ye, J., Yang, X.,  
636 Tao, S., Liu, H., and Yao, W.: Dissecting the contributions of organic nitrogen aerosols  
637 to global atmospheric nitrogen deposition and implications for ecosystems, *Natl. Sci.*  
638 *Rev.*, 10, <https://doi.org/10.1093/nsr/nwad244>, 2023.

639 Liu, Q., Liu, Y., Zhao, Q., Zhang, T., and Schauer, J. J.: Increases in the formation of water  
640 soluble organic nitrogen during Asian dust storm episodes, *Atmos. Res.*, 253, 105486,  
641 <https://doi.org/10.1016/j.atmosres.2021.105486>, 2021.

642 Liu, X., Wang, H., Wang, F., Lv, S., Wu, C., Zhao, Y., Zhang, S., Liu, S., Xu, X., Lei, Y., and  
643 Wang, G.: Secondary Formation of Atmospheric Brown Carbon in China Haze:  
644 Implication for an Enhancing Role of Ammonia, *Environ. Sci. Technol.*, 57, 11163-11172,  
645 <https://doi.org/10.1021/acs.est.3c03948>, 2023.

646 Luo, L., Kao, S. J., Bao, H., Xiao, H., Xiao, H., Yao, X., Gao, H., Li, J., and Lu, Y.: Sources  
647 of reactive nitrogen in marine aerosol over the Northwest Pacific Ocean in spring, *Atmos.*  
648 *Chem. Phys.*, 18, 6207-6222, <https://doi.org/10.5194/acp-18-6207-2018>, 2018.

649 Mace, K. A., Duce, R. A., and Tindale, N. W.: Organic nitrogen in rain and aerosol at Cape  
650 Grim, Tasmania, Australia, *J. Geophys. Res.-Atmos.*, 108,  
651 <https://doi.org/10.1029/2002JD003051>, 2003.

652 Matsumoto, K., Kobayashi, H., Hara, K., Ishino, S., and Hayashi, M.: Water-soluble organic  
653 nitrogen in fine aerosols over the Southern Ocean, *Atmos. Environ.*, 287,  
654 <https://doi.org/10.1016/j.atmosenv.2022.119287>, 2022.

655 Matsumoto, K., Sakata, K., and Watanabe, Y.: Water-soluble and water-insoluble organic  
656 nitrogen in the dry and wet deposition, *Atmos. Environ.*, 218,  
657 <https://doi.org/10.1016/j.atmosenv.2019.117022>, 2019a.

658 Matsumoto, K., Watanabe, Y., Horiuchi, K., and Nakano, T.: Simultaneous measurement  
659 of the water-soluble organic nitrogen in the gas phase and aerosols at a forested site in  
660 Japan, *Atmos. Environ.*, 200, 312-318, <https://doi.org/10.1016/j.atmosenv.2018.12.011>,  
661 2019b.

662 Matsumoto, K., Yamamoto, Y., Kobayashi, H., Kaneyasu, N., and Nakano, T.: Water-  
663 soluble organic nitrogen in the ambient aerosols and its contribution to the dry deposition  
664 of fixed nitrogen species in Japan, *Atmos. Environ.*, 95, 334-343,

665 <https://doi.org/10.1016/j.atmosenv.2014.06.037>, 2014.

666 Matsumoto, K., and Yamato, K.: Uncertainties in the measurements of water-soluble  
667 organic nitrogen in the aerosol, *Atmos. Environ.*, 144, 220-225,  
668 <https://doi.org/10.1016/j.atmosenv.2016.08.061>, 2016.

669 Miyazaki, Y., Fu, P., Ono, K., Tachibana, E., and Kawamura, K.: Seasonal cycles of water-  
670 soluble organic nitrogen aerosols in a deciduous broadleaf forest in northern Japan, *J.*  
671 *Geophys. Res.-Atmos.*, 119, 1440-1454, <https://doi.org/10.1002/2013jd020713>, 2014.

672 Miyazaki, Y., Kawamura, K., Jung, J., Furutani, H., and Uematsu, M.: Latitudinal  
673 distributions of organic nitrogen and organic carbon in marine aerosols over the western  
674 North Pacific, *Atmos. Chem. Phys.*, 11, 3037-3049, [https://doi.org/10.5194/acp-11-3037-](https://doi.org/10.5194/acp-11-3037-2011)  
675 2011, 2011.

676 Nehir, M., and Koçak, M.: Atmospheric water-soluble organic nitrogen (WSON) in the  
677 eastern Mediterranean: origin and ramifications regarding marine productivity, *Atmos.*  
678 *Chem. Phys.*, 18, 3603-3618, <https://doi.org/10.5194/acp-18-3603-2018>, 2018.

679 Norris, G., Duvall, R., Brown, S., and Bai, S.: EPA Positive Matrix Factorization (PMF) 5.0  
680 fundamentals and User Guide Prepared for the US Environmental Protection Agency  
681 Office of Research and Development, Washington, DC, 2014.

682 O'Dowd, C. D., Facchini, M. C., Cavalli, F., Ceburnis, D., Mircea, M., Decesari, S., Fuzzi,  
683 S., Yoon, Y. J., and Putaud, J.-P.: Biogenically driven organic contribution to marine  
684 aerosol, *Nature*, 431, 676-680, <https://doi.org/10.1038/nature02959>, 2004.

685 O'Dowd, C., Ceburnis, D., Ovadnevaite, J., Bialek, J., Stengel, D. B., Zacharias, M.,  
686 Nitschke, U., Connan, S., Rinaldi, M., Fuzzi, S., Decesari, S., Cristina Facchini, M.,  
687 Marullo, S., Santoleri, R., Dell'Anno, A., Corinaldesi, C., Tangherlini, M., and Danovaro,  
688 R.: Connecting marine productivity to sea-spray via nanoscale biological processes:  
689 Phytoplankton Dance or Death Disco?, *Sci Rep*, 5, 14883,  
690 <https://doi.org/10.1038/srep14883>, 2015.

691 Park, K.-T., Lee, K., Kim, T.-W., Yoon, Y. J., Jang, E.-H., Jang, S., Lee, B.-Y., and  
692 Hermansen, O.: Atmospheric DMS in the Arctic Ocean and Its Relation to Phytoplankton  
693 Biomass, *Global Biogeochem. Cycles*, 32, 351-359,  
694 <https://doi.org/10.1002/2017GB005805>, 2018.

695 Pavuluri, C. M., Kawamura, K., and Fu, P. Q.: Atmospheric chemistry of nitrogenous  
696 aerosols in northeastern Asia: biological sources and secondary formation, *Atmos.*  
697 *Chem. Phys.*, 15, 9883-9896, <https://doi.org/10.5194/acp-15-9883-2015>, 2015.

698 Pryor, S. C., and Sørensen, L. L.: Nitric Acid–Sea Salt Reactions: Implications for Nitrogen  
699 Deposition to Water Surfaces, *J. Appl. Meteorol.*, 39, 725-731,  
700 <https://doi.org/10.1175/1520-0450-39.5.725>, 2000.

701 Prather, K. A., Bertram, T. H., Grassian, V. H., Deane, G. B., Stokes, M. D., DeMott, P. J.,  
702 Aluwihare, L. I., Palenik, B. P., Azam, F., Seinfeld, J. H., Moffet, R. C., Molina, M. J.,  
703 Cappa, C. D., Geiger, F. M., Roberts, G. C., Russell, L. M., Ault, A. P., Baltrusaitis, J.,  
704 Collins, D. B., Corrigan, C. E., Cuadra-Rodriguez, L. A., Ebben, C. J., Forestieri, S. D.,  
705 Guasco, T. L., Hersey, S. P., Kim, M. J., Lambert, W. F., Modini, R. L., Mui, W., Pedler,  
706 B. E., Ruppel, M. J., Ryder, O. S., Schoepp, N. G., Sullivan, R. C., and Zhao, D.: Bringing

707 the ocean into the laboratory to probe the chemical complexity of sea spray aerosol,  
708 Proc. Natl. Acad. Sci. U. S. A., 110, 7550-7555,  
709 <https://doi.org/10.1073/pnas.1300262110>, 2013.

710 Quinn, P. K., Bates, T. S., Schulz, K. S., Coffman, D. J., Frossard, A. A., Russell, L. M.,  
711 Keene, W. C., and Kieber, D. J.: Contribution of sea surface carbon pool to organic  
712 matter enrichment in sea spray aerosol, Nat. Geosci., 7, 228-232,  
713 <https://doi.org/10.1038/ngeo2092>, 2014.

714 Rinaldi, M., Fuzzi, S., Decesari, S., Marullo, S., Santolero, R., Provenzale, A., von  
715 Hardenberg, J., Ceburnis, D., Vaishya, A., O'Dowd, C. D., and Facchini, M. C.: Is  
716 chlorophyll-a the best surrogate for organic matter enrichment in submicron primary  
717 marine aerosol?, J. Geophys. Res.-Atmos., 118, 4964-4973,  
718 <https://doi.org/10.1002/jgrd.50417>, 2013.

719 Savoie, D. L., Arimoto, R., Keene, W. C., Prospero, J. M., Duce, R. A., and Galloway, J. N.:  
720 Marine biogenic and anthropogenic contributions to non-sea-salt sulfate in the marine  
721 boundary layer over the North Atlantic Ocean, J. Geophys. Res.-Atmos., 107, 4356,  
722 <https://doi.org/10.1029/2001JD000970>, 2002.

723 Schiffer, J. M., Mael, L. E., Prather, K. A., Amaro, R. E., and Grassian, V. H.: Sea Spray  
724 Aerosol: Where Marine Biology Meets Atmospheric Chemistry, ACS Central Sci., 4,  
725 1617-1623, <https://doi.org/10.1021/acscentsci.8b00674>, 2018.

726 Sciare, J., Favez, O., Sarda-Estève, R., Oikonomou, K., Cachier, H., and Kazan, V.: Long-  
727 term observations of carbonaceous aerosols in the Austral Ocean atmosphere: Evidence  
728 of a biogenic marine organic source, J. Geophys. Res.-Atmos., 114,  
729 <https://doi.org/10.1029/2009JD011998>, 2009.

730 Shi, J., Gao, H., Qi, J., Zhang, J., and Yao, X.: Sources, compositions, and distributions of  
731 water-soluble organic nitrogen in aerosols over the China Sea, J. Geophys. Res.-Atmos.,  
732 115, <https://doi.org/10.1029/2009JD013238>, 2010.

733 Sun, Y. L., Zhang, Q., Schwab, J. J., Chen, W. N., Bae, M. S., Lin, Y. C., Hung, H. M., and  
734 Demerjian, K. L.: A case study of aerosol processing and evolution in summer in New  
735 York City, Atmos. Chem. Phys., 11, 12737-12750, [https://doi.org/10.5194/acp-11-12737-](https://doi.org/10.5194/acp-11-12737-2011)  
736 2011, 2011.

737 Tang, J., Hu, S., Wang, X., Wang, J., Lv, S., Geng, X., Zhong, G., Mo, Y., Bualert, S., Li, J.,  
738 Zhao, S., and Zhang, G.: Data and code for "Marine-Derived Water-Soluble Organic  
739 Nitrogen in Coastal Air: Influence of Ocean Productivity on Atmospheric Nitrogen  
740 Cycling", OSF, <https://doi.org/10.17605/OSF.IO/YMJ3F>, 2026.

741 Tang, J., Wang, J., Zhong, G., Jiang, H., Mo, Y., Zhang, B., Geng, X., Chen, Y., Tang, J.,  
742 Tian, C., Bualert, S., Li, J., and Zhang, G.: Measurement report: Long-emission-  
743 wavelength chromophores dominate the light absorption of brown carbon in aerosols  
744 over Bangkok: impact from biomass burning, Atmos. Chem. Phys., 21, 11337-11352,  
745 <https://doi.org/10.5194/acp-21-11337-2021>, 2021.

746 Tang, J., Xu, B., Zhao, S., Li, J., Tian, L., Geng, X., Jiang, H., Mo, Y., Zhong, G., Jiang, B.,  
747 Chen, Y., Tang, J., and Zhang, G.: Long-Emission-Wavelength Humic-Like Component  
748 (L-HULIS) as a Secondary Source Tracer of Brown Carbon in the Atmosphere, J.

749 Geophys. Res.-Atmos., 129, e2023JD040144, <https://doi.org/10.1029/2023JD040144>,  
750 2024.

751 Tian, M., Li, H., Wang, G., Fu, M., Qin, X., Lu, D., Liu, C., Zhu, Y., Luo, X., Deng, C.,  
752 Abdullaev, S. F., and Huang, K.: Seasonal source identification and formation processes  
753 of marine particulate water soluble organic nitrogen over an offshore island in the East  
754 China Sea, *Sci. Total Environ.*, 863, 160895,  
755 <https://doi.org/10.1016/j.scitotenv.2022.160895>, 2023.

756 Tripathee, L., Kang, S., Chen, P., Bhattarai, H., Guo, J., Shrestha, K. L., Sharma, C. M.,  
757 Sharma Ghimire, P., and Huang, J.: Water-soluble organic and inorganic nitrogen in  
758 ambient aerosols over the Himalayan middle hills: Seasonality, sources, and transport  
759 pathways, *Atmos. Res.*, 250, 105376, <https://doi.org/10.1016/j.atmosres.2020.105376>,  
760 2021.

761 Tsagkaraki, M., Theodosi, C., Grivas, G., Vargiakaki, E., Sciare, J., Savvides, C., and  
762 Mihalopoulos, N.: Spatiotemporal variability and sources of aerosol water-soluble  
763 organic nitrogen (WSON), in the Eastern Mediterranean, *Atmos. Environ.*, 246, 118144,  
764 <https://doi.org/10.1016/j.atmosenv.2020.118144>, 2021.

765 Violaki, K., Sciare, J., Williams, J., Baker, A. R., Martino, M., and Mihalopoulos, N.:  
766 Atmospheric water-soluble organic nitrogen (WSON) over marine environments: a  
767 global perspective, *Biogeosciences*, 12, 3131-3140, [https://doi.org/10.5194/bg-12-3131-](https://doi.org/10.5194/bg-12-3131-2015)  
768 2015, 2015.

769 Wang, G. H., Cheng, C. L., Huang, Y., Tao, J., Ren, Y. Q., Wu, F., Meng, J. J., Li, J. J.,  
770 Cheng, Y. T., Cao, J. J., Liu, S. X., Zhang, T., Zhang, R., and Chen, Y. B.: Evolution of  
771 aerosol chemistry in Xi'an, inland China, during the dust storm period of 2013–Part 1:  
772 Sources, chemical forms and formation mechanisms of nitrate and sulfate, *Atmos. Chem.*  
773 *Phys.*, 14, 11571-11585, <https://doi.org/10.5194/acp-14-11571-2014>, 2014.

774 Wang, J., Jiang, H., Jiang, H., Mo, Y., Geng, X., Li, J., Mao, S., Bualert, S., Ma, S., Li, J.,  
775 and Zhang, G.: Source apportionment of water-soluble oxidative potential in ambient  
776 total suspended particulate from Bangkok: Biomass burning versus fossil fuel  
777 combustion, *Atmos. Environ.*, 235, 117624,  
778 <https://doi.org/10.1016/j.atmosenv.2020.117624>, 2020.

779 Xie, M., Chen, X., Hays, M. D., Lewandowski, M., Offenberg, J., Kleindienst, T. E., and  
780 Holder, A. L.: Light Absorption of Secondary Organic Aerosol: Composition and  
781 Contribution of Nitroaromatic Compounds, *Environ. Sci. Technol.*, 51, 11607-11616,  
782 <https://doi.org/10.1021/acs.est.7b03263>, 2017.

783 Xing, J., Song, J., Yuan, H., Wang, Q., Li, X., Li, N., Duan, L., and Qu, B.: Water-soluble  
784 nitrogen and phosphorus in aerosols and dry deposition in Jiaozhou Bay, North China:  
785 Deposition velocities, origins and biogeochemical implications, *Atmos. Res.*, 207, 90-99,  
786 <https://doi.org/10.1016/j.atmosres.2018.03.001>, 2018.

787 Xu, Y., Miyazaki, Y., Tachibana, E., Sato, K., Ramasamy, S., Mochizuki, T., Sadanaga, Y.,  
788 Nakashima, Y., Sakamoto, Y., Matsuda, K., and Kajii, Y.: Aerosol Liquid Water Promotes  
789 the Formation of Water-Soluble Organic Nitrogen in Submicrometer Aerosols in a  
790 Suburban Forest, *Environ. Sci. Technol.*, 54, 1406-1414,

791 <https://doi.org/10.1021/acs.est.9b05849>, 2020.

792 Yu, X., Pan, Y., Song, W., Li, S., Li, D., Zhu, M., Zhou, H., Zhang, Y., Li, D., Yu, J., Wang,  
793 X., and Wang, X.: Wet and Dry Nitrogen Depositions in the Pearl River Delta, South  
794 China: Observations at Three Typical Sites With an Emphasis on Water-Soluble Organic  
795 Nitrogen, *J. Geophys. Res.-Atmos.*, 125, <https://doi.org/10.1029/2019jd030983>, 2020.

796 Yu, X., Yu, Q., Zhu, M., Tang, M., Li, S., Yang, W., Zhang, Y., Deng, W., Li, G., Yu, Y., Huang,  
797 Z., Song, W., Ding, X., Hu, Q., Li, J., Bi, X., and Wang, X.: Water Soluble Organic  
798 Nitrogen (WSO<sub>N</sub>) in Ambient Fine Particles Over a Megacity in South China:  
799 Spatiotemporal Variations and Source Apportionment, *J. Geophys. Res.-Atmos.*, 122,  
800 13,045-13,060, <https://doi.org/10.1002/2017JD027327>, 2017.

801 Zamora, L. M., Prospero, J. M., and Hansell, D. A.: Organic nitrogen in aerosols and  
802 precipitation at Barbados and Miami: Implications regarding sources, transport and  
803 deposition to the western subtropical North Atlantic, *J. Geophys. Res.-Atmos.*, 116,  
804 <https://doi.org/10.1029/2011JD015660>, 2011.

805 Zhao, Y., Bao, Z., Long, X., Liu, Y., Han, Y., Meng, L., Zeng, X., Li, L., Qi, X., Li, Z., Peng,  
806 C., Zhang, L., Chen, M., Zhai, C., and Chen, Y.: Evolution of secondary organic aerosol  
807 under extremely high humidity conditions in urban areas of southwestern China:  
808 Formation and scavenging, *Atmos. Res.*, 327, 108318,  
809 <https://doi.org/10.1016/j.atmosres.2025.108318>, 2026.

810 Zhou, S., Chen, Y., Paytan, A., Li, H., Wang, F., Zhu, Y., Yang, T., Zhang, Y., and Zhang,  
811 R.: Non-Marine Sources Contribute to Aerosol Methanesulfonate Over Coastal Seas, *J.*  
812 *Geophys. Res.-Atmos.*, 126, e2021JD034960, <https://doi.org/10.1029/2021JD034960>,  
813 2021.

814 Zhou, S., Chen, Y., Wang, F., Bao, Y., Ding, X., and Xu, Z.: Assessing the Intensity of Marine  
815 Biogenic Influence on the Lower Atmosphere: An Insight into the Distribution of Marine  
816 Biogenic Aerosols over the Eastern China Seas, *Environ. Sci. Technol.*, 57, 12741-12751,  
817 <https://doi.org/10.1021/acs.est.3c04382>, 2023.

818

819